Open

Cell Death and Differentiation (2012) 19, 839–846

www.nature.com/cdd

Overlapping functions of microRNAs in control of apoptosis during *Drosophila* embryogenesis

W Ge[1], Y-W Chen[1], R Weng[1], SF Lim[1], M Buescher[1], R Zhang[2] and SM Cohen*[,1,3]

Regulation of apoptosis is crucial for tissue homeostasis under normal development and environmental stress. In *Drosophila*, cell death occurs in different developmental processes including embryogenesis. Here, we report that two members of the miR-2 seed family of microRNAs, *miR-6* and *miR-11*, function together to limit the level of apoptosis during *Drosophila* embryonic development. Mutants lacking both *miR-6* and *miR-11* show embryonic lethality and defects in the central nervous system (CNS). We provide evidence that *miR-6/11* functions through regulation of the proapoptotic genes, *reaper* (*rpr*), *head involution defective* (*hid*), *grim* and *sickle* (*skl*). Upregulation of these proapoptotic genes is responsible for the elevated apoptosis and the CNS defects in the mutants. These findings demonstrate that the activity of the proapoptotic genes is kept in check by *miR-6/11* to ensure normal development.
Cell Death and Differentiation (2012) **19,** 839–846; doi:10.1038/cdd.2011.161; published online 18 November 2011

Apoptosis is an important regulatory mechanism during growth development of animal embryos, and in disease. Cell proliferation is intimately linked with cell death. Cues that drive cell growth and division also induce apoptosis. Overcoming the apoptosis barrier is a critical step in the ability of cancers to grow *in vivo*.[1,2] Many of the signaling pathways implicated in the normal control of tissue growth during animal development have been found to coordinate cell proliferation and apoptosis. For example, the Hippo signaling pathway has an evolutionarily conserved role in controlling tissue growth rates and organ size during animal development and mutations that cause a net gain of function can lead to cancer.[3]

In *Drosophila*, apoptotic inputs converge to a common death program through the activation of the proapoptotic genes: *reaper* (*rpr*), *grim*, *head involution defective* (*hid*) and *sickle* (*skl*). The proapoptotic activity of the protein products of these four genes results from their ability to bind and inactivate the Drosophila Inhibitor of Apoptosis (DIAP), which in turn inhibits Caspases.[4] Activity of the proapoptotic genes has been identified as a key target of many signaling pathways that regulate growth and patterning in *Drosophila*. Targets of the Hippo signaling pathway include regulators of cell proliferation, including *cycE* and *myc*,[5,6] as well as regulators of apoptosis, including *DIAP* and the antiapoptotic *bantam* miRNA.[3,7,8] Signaling via the MAPK pathway also controls *hid* expression and activity.[9,10] In addition, environmental stress such as, UV and X-ray can activate the DNA damage p53 pathway to regulate expression of *rpr*.[11–14] Wingless signaling activates the expression of *hid*, *rpr* and *grim* to induce apoptosis in eye development.[15,16] The steroid hormone ecdysone signaling is required for the induction of *rpr* and *hid* during metamorphosis.[17]

Emerging evidence has shown that miRNAs have a key role in controlling apoptosis to maintain the balance of cell life and death by targeting proapoptotic or antiapoptotic genes. For instance, miR-21 functions as an antiapoptotic factor in many different cancer cells.[18–20] The miR-34 microRNA family can induce apoptosis and its expression is upregulated in many tumor types.[21] miR-24a has also been reported to target the proapoptotic factors caspase9 and apaf1 to limit the level of apoptosis during retina development.[22] In *Drosophila*, the *bantam* and *miR263a/b* miRNAs regulate apoptosis by controlling *hid* expression.[23,24] Previous reports have suggested that microRNAs of the *miR-2* seed family can regulate expression of *rpr*, *grim* and *skl*.[25–27] These studies have raised the possibility that the normal function of these miRNAs might be to control apoptosis *in vivo*. Here, we examine this possibility using targeted homologous recombination to generate mutants removing activity of *miR-11* and explore the *in vivo* functions of the miR-6/miR-11 subgroup of the miR-2 seed family. These studies provide evidence for partially redundant functions in control of apoptosis for *miR-6* and *miR-11* during development of the embryonic central nervous system (CNS).

Results

Generation and characterization of *miR-11* mutant alleles. To explore the functions of the members of the miR-2 family we have generated mutants that remove miRNA function. The miR-2 seed family contains 13 precursor miRNAs, which generate 8 different mature miRNAs (Figure 1a). The 8 mature miRNAs could fall into two subgroups according to 3′ portion similarity: the miR-2/13 group and the miR-6/11 group (Figure 1b). We previously reported a mutation that removes

[1]Institute of Molecular Cell Biology, 61 Biopolis Drive, Singapore 138673, Singapore; [2]Beijing Institute of Genomics, Chinese Academy of Sciences, Beijing 100029, China and [3]Department of Biological Sciences, National University of Singapore, Singapore, Singapore
*Corresponding author: SM Cohen, Department of Biological Sciences, Institute for Molecular Cell Biology, National University of Singapore, 61 Biopolis Drive, Singapore 138673, Singapore. Tel: +65 6586 8725; E-mail: scohen@imcb.a-star.edu.sg
Keywords: microRNA; central nervous system; miR-6; miR-11; miR-2
Abbreviations: rpr, reaper; hid, head involution defective; skl, sickle; DIAP, Drosophila Inhibitor of Apoptosis
Received 16.5.11; revised 06.9.11; accepted 16.9.11; Edited by E Baehrecke; published online 18.11.11

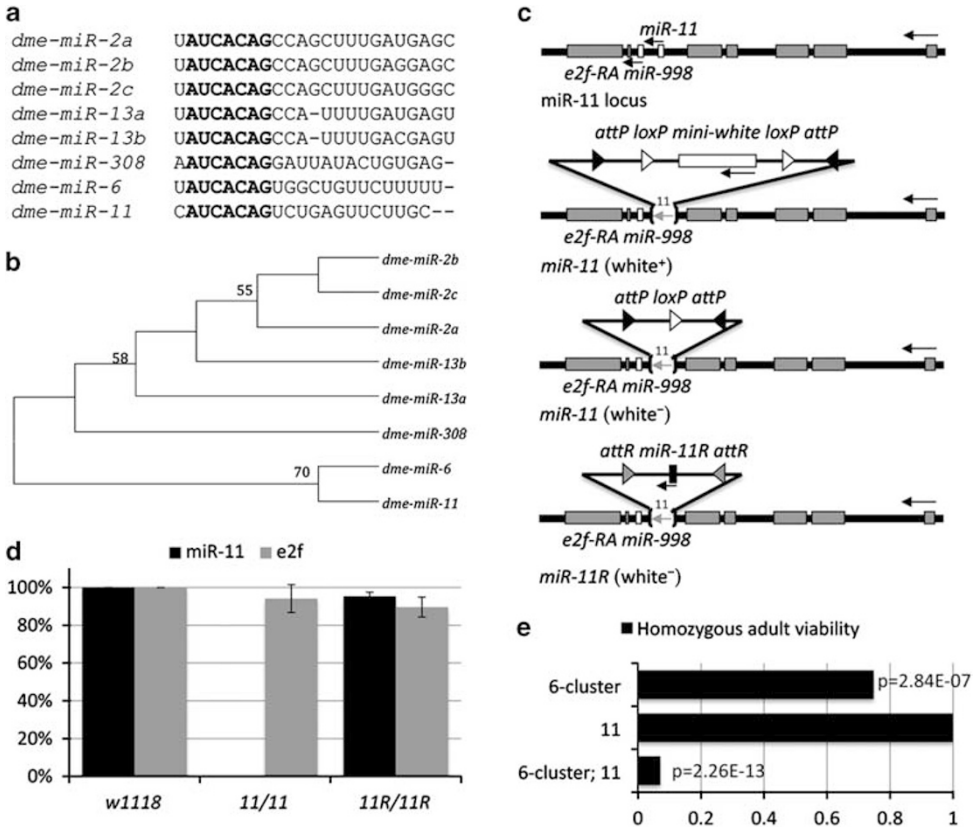

Figure 1 The *miR-11* mutant. (**a**) Sequence alignment of *Drosophila* miR-2 family miRNAs. The seed region is shown in bold. (**b**) Phylogenetic analysis to show the evolutionary relationships among *Drosophila* miR-2 seed family miRNAs. The tree was reconstructed using the neighbor-joining method. The bootstrap values >50 are shown above the branches. (**c**) Diagrams of the *miR-11* locus illustrating the structures of the locus at different stages of gene targeting. Gray boxes indicate exons of the *E2F* gene. White boxes indicate the positions of miR-11 and miR-998. Arrows indicate the direction of transcription. In the second diagram the bracketed area indicates the DNA removed including miR-11. The integrated DNA is shown above. Filled triangles indicate AttP sites. Open triangles indicate LoxP sites. The open box indicates the *mini-white* reporter used to provide a genetic eye-color marker. *mini-white* contains introns (not shown). The third diagram shows the structure of the targeted locus after excision of the *mini-white* cassette by use of Cre recombinase to delete the DNA between the LoxP sites. The fourth diagram shows the product of the RMCE-mediated replacement of the *mini-white* cassette with miR-11 genomic DNA. (**d**) Histogram showing the levels of *miR-11* miRNA and *E2F* mRNA measured by quantitative RT-PCR. RNA was extracted from w^{1118} control flies, $miR\text{-}11^{(w-)}$ homozygous mutants (diagram 3 of panel **c**) and from rescued $miR\text{-}11R^{(w-)}$ homozygous flies (diagram 4 of panel **c**). Error bars represent standard deviation from three independent experiments. (**e**) Histogram showing the survival rates of the homozygous *miR-6* cluster mutant, homozygous *miR-11* mutant and the doubly homozygous *miR-6 cluster miR-11* mutant flies. *miR-11* mutants were not different from controls (not shown). Fisher's exact test was used to assess the significance of the reduced survival of the mutants

the three genomic copies of *miR-6*, along with 5 other miRNAs,[28] referred to here as the *miR-6-cluster*). Figure 1c illustrates the targeting strategy used to knockout the closely related *miR-11* gene.

miR-11 is located in an intron of the *E2F* gene, which encodes a cell cycle transcription factor. The targeting strategy involved replacing *miR-11* sequences with a *mini-white* reporter gene flanked by loxP sites and by inverted *attP* sites to allow recombinase mediated cassette exchange (RMCE)[29] at the targeted locus (as described in Weng *et al.*[30]). Introns in the *mini-white* gene are expected to disrupt splicing of the host gene E2F. We confirmed that this was the case by crossing the *miR-11* targeted allele $miR\text{-}11^{KO\ (w+)}$ to a null allele of *E2F*.[31] The combination was semi-lethal, indicating disruption of *E2F* function. To generate an allele of *miR-11* that did not impair *E2F* function, the *mini-white* cassette was excised by expression of Cre recombinase. The resulting allele lacked the *mini-white* marker, but retains a single LoxP site in the intron, as well as the inverted *attP* sites (Figure 1c, third diagram). Quantitative RT-PCR analysis showed that the miR-11 miRNA was absent in RNA samples from the homozygous $miR\text{-}11^{KO\ (w-)}$ mutant (Figure 1d). We made use of the inverted *attP* sites to prepare a genetic rescue using RMCE to replace the *miR-11* hairpin back into the targeted locus (Figure 1c, fourth diagram). The rescue construct restored miR-11 RNA to $\sim$90% of the control levels (Figure 1d).

As the *miR-11* locus is located in the intron of *E2F* we wanted to determine whether the effects of the mutant alleles could be cleanly attributed to loss of *miR-11*. Quantitative RT-PCR, using exon specific primers showed that mature spliced *E2F* mRNA levels were near normal in the homozygous $miR\text{-}11^{\ KO\ (w-)}$ mutant (Figure 1d). When crossed to a null allele of *E2F*, the $miR\text{-}11^{KO\ (w-)}/E2F$ trans-heterozygous combination was viable. Thus the $miR\text{-}11^{KO\ (w-)}$ allele does not meaningfully impair function of the E2F gene.

Overlapping roles of *miR-11* and *miR-6*. As reported previously, a deletion removing the *miR-6* cluster, which contains

the three *miR-6* genes, showed a modest reduction in viability to adulthood[28] (confirmed in Figure 1e). *miR-11* mutants were normally viable. However, the *miR-6*, *miR-11* double mutant combination showed a strong reduction in survival to adulthood (Figure 1e). This suggests that *miR-11* and the *miR-6* cluster may have partially overlapping functions during *Drosophila* development. To explore these functions in more detail we examined combinations of these mutants for their ability to complete embryogenesis.

miR-6 expression is undetectable during oogenesis, but is transcriptionally upregulated at the onset of zygotic transcription in the blastoderm-stage embryo and continues to be expressed throughout embryonic development.[28,32] As a consequence we do not expect maternal contribution of *miR-6* to support its function in the embryo. In contrast, *miR-11* is the thirteenth most abundant miRNA in ovaries,[33] allowing for the possibility that maternally provided *miR-11* could suffice for embryonic development. Homozygous *miR-11* mutants showed no significant reduction in the completion of embryogenesis compared with controls (Figure 2a). Similarly, homozygous *miR-6* cluster deletion mutants showed little or no effect. We noted that removing one copy of *miR-11* in the *miR-6* cluster mutant background resulted in a modest but statistically significant decrease in survival (Figure 2a). The reciprocal combination, removing one copy of *miR-6* cluster in the *miR-11* homozygous mutant background did not significantly affect survival.

The *miR-6/11* double mutant combination showed strong embryonic lethality (Figure 2a). This lethality could be rescued by restoring expression of *miR-11* in the double mutant

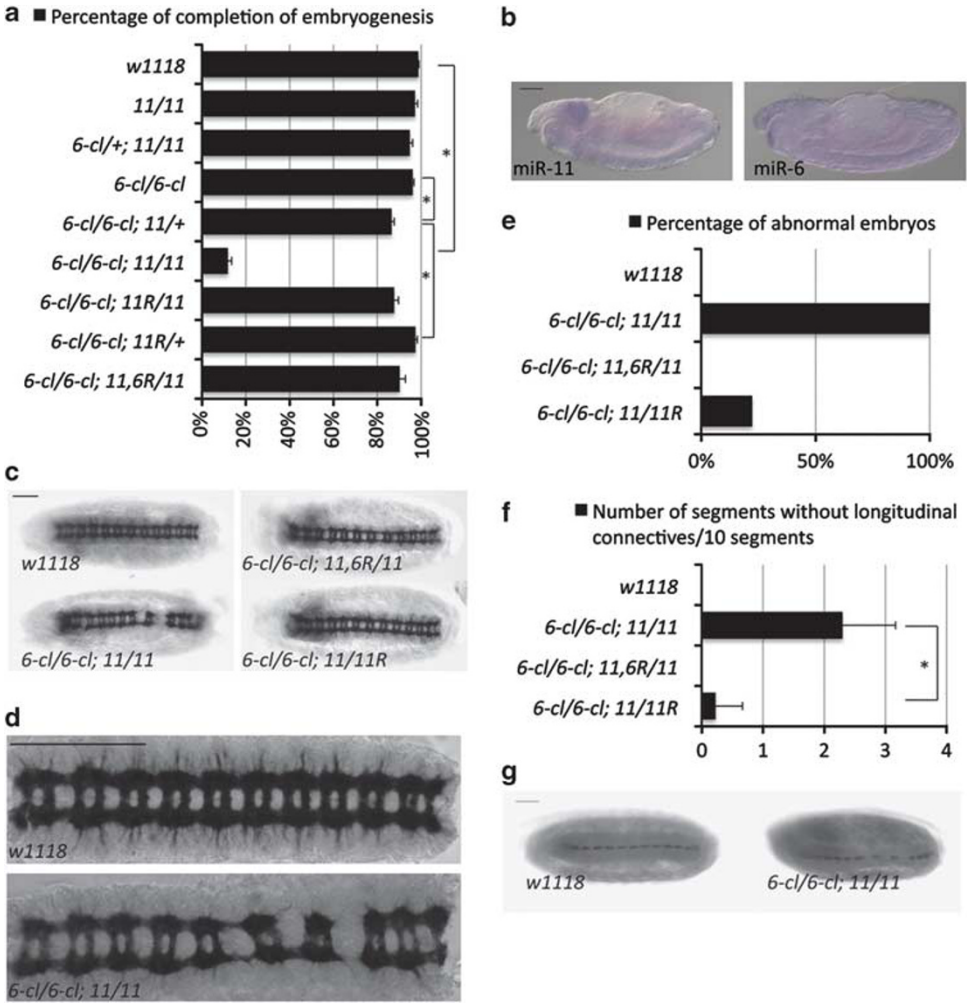

Figure 2 Embryonic phenotypes of *miR-6/miR-11* double mutants. (**a**) Histogram showing percentage of embryos that completed embryonic development, assessed by hatching to first instar larval stage. Error bars represent standard deviation from three independent experiments. Student's *t*-test was used to assess the significance of the differences indicated. $*P<0.05$. (**b**) Lateral views of embryos labeled by *in situ* hybridization to detect the primary transcript of *miR-11* and *miR-6* miRNAs. Scale bar: 50 μm. (**c**) Ventral views of embryos of the indicated genotypes labeled with antibody BP102. BP102 labels the axonal scaffold of the CNS. *11*, *6R* denotes the *miR-11* mutant chromosome carrying the rescue transgene for *miR-6*. *11R* denotes the RMCE-rescued version of the *miR-11* mutant. Scale bar: 50 μm. (**d**) Higher magnification view to highlight the defects in the CNS. Scale bar: 50 μm. (**e**, **f**) Histograms showing quantification of the defects in the mutants and the rescued mutants. (**e**) Percentage of embryos affected in at least one segment of the CNS. (**f**) Average number of affected segments per 10 segments scored. w^{1118} indicates the genotype of the control flies. Error bars represent standard deviation from at least eight embryos. * indicates that the difference between the indicated pair was statistically significant $P<0.05$ (Student's *t*- test). (**g**) Ventral views of embryos of the indicated genotypes labeled with anti-Wrapper. Wrapper labels the midline glia of the CNS. Scale bar: 50 μm

background using the *miR-11*^{R} allele. The *miR-11*^{R} allele was made by reintroducing *miR-11* sequences back into the targeted *miR-11*^{KO} mutant chromosome, using RMCE. Reconstructing a functional *miR-11* locus in the mutant chromosome provides a consistent genetic background for the comparison. Unlike the original *miR-11*^{KO} mutant chromosome, introducing one copy of the *miR-11*^{R} chromosome did not affect survival of the *miR-6* mutant (Figure 2a; there was no significant difference between *miR-6* mutants with two normal alleles of *miR-11 versus* one normal allele/*miR-11*^{R}). Restoring *miR-6* activity in the double mutant combination by introduction of a rescue transgene expressing *miR-6* under control of its endogenous promoter was also sufficient to rescue the lethality of the double mutant (Figure 2a). The transgene expressed *miR-6*, but not the other members of the cluster: *miR-3*, *miR-4*, *miR-5*, *miR-286* and *miR-309*. This indicates that the absence of the other 5 miRNAs is not responsible for the lethality of the double mutant. These data suggest that *miR-11* and *miR-6* have overlapping functions during embryogenesis. Consistent with this proposal, these miRNAs are broadly coexpressed in the embryo, with miR-11 showing slightly elevated expression in the embryonic CNS (Figure 2b).

Embryonic CNS defects in *miR-6/miR-11* double mutants. Having established that the *miR-11 miR-6* double mutant combination shows reduced survival during embryonic development, we examined the mutants for the evidence of defects that could be associated with lethality. There was no indication for reproducible defects in the patterning or differentiation of epidermal cuticle or of the head skeleton, suggesting that major processes of morphogenesis proceeded more or less normally in the mutants. However, a reproducible defect was observed in the organization of the embryonic CNS, using BP102 antibody to label the axonal scaffold of the CNS (Figures 2c and d). Longitudinal connectives were thin and showed occasional gaps between segments, typically interrupting the nerve cord in the mid-abdominal region. Commissures were also abnormal in spacing and thickness. In all 100% of double mutant embryos showed abnormal CNS morphology in at least one segment (Figure 2e). On an average 2 segments per embryo lacked longitudinal connectives (Figure 2f). These defects were not observed in double mutant embryos rescued by inclusion of the *miR-6* rescue transgene, and were considerably less frequent in double mutant embryos rescued by inclusion of the rescue allele *miR-11*^{R} (Figures 2e and f).

To examine the CNS axonal scaffold phenotype in more detail, we asked if the midline glial cells were affected in the double mutant embryos. Midline glia has a key role in organization of the axon scaffold.[34] Embryos were labeled with antibody to the midline glia-specific marker Wrapper, a member of the immunoglobulin superfamily.[35] Wrapper-expressing cells were irregular in shape and spacing, and in some cases were lost in the affected region of the double mutant embryos (Figure 2g).

***miR-6/miR-11* double mutant phenotypes due to elevated apoptosis.** The observed defects in the CNS development would be consistent with elevated apoptosis. Antibody labeling to visualize the activated form of Caspase 3 showed elevated Caspase activity in the double mutant embryos (Figure 3a). Previous reports have suggested that members of the miR-2 seed family can regulate the expression of proapoptotic genes, including *rpr*, *grim* and *skl*.[25–27] We therefore sought to measure the expression of the proapoptotic genes in *miR-6/miR-11* double mutant embryos. Quantitative RT-PCR showed that *rpr*, *grim, skl* and *hid* were upregulated by 2–4 fold in RNA samples from *miR-6/miR-11* double mutant embryos (Figure 3b).

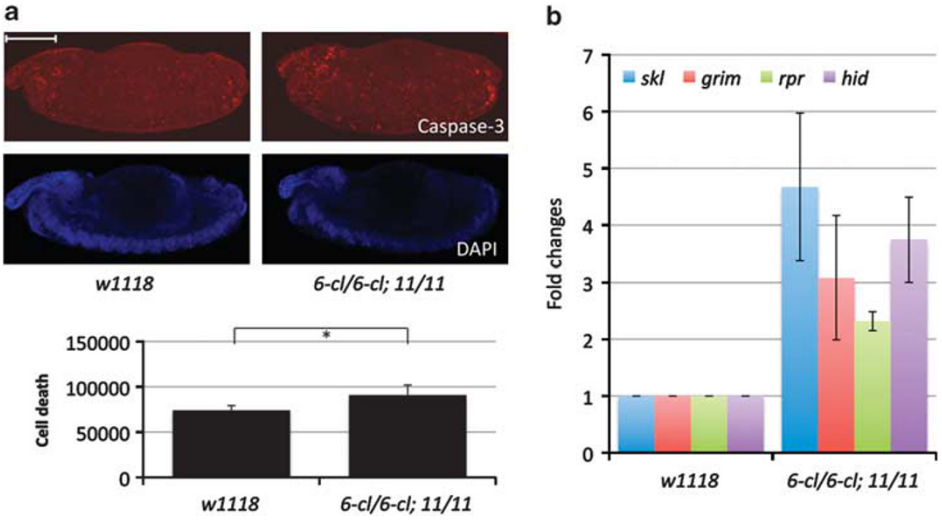

Figure 3 Regulation of proapoptotic genes by *miR-6/miR-11*. (**a**) Lateral views of embryos labeled with antibody to the activated form of Caspase 3 (red) and with DAPI (blue). Scale bar: 50 μm. Stacks of confocal sections were used to create 3D-reconstructions with the 'isosurface' module of Imaris software and the total enclosed volume was measured as a surrogate to quantify apoptosis (arbitrary units in the histogram). Error bars represent standard deviation from analysis of four embryos of each genotype. * indicates that the difference was statistically significant, $P<0.05$ (Student's *t*-test). Scale bar: 100 μm. (**b**) Histogram showing the levels of *rpr*, *grim*, *hid* and *skl* mRNAs measured by quantitative RT-PCR. RNA was extracted from w^{1118} control embryos and embryos doubly mutant for *mir-6-cluster* and *miR-11*$^{(w-)}$. Error bars represent standard deviation from three independent experiments

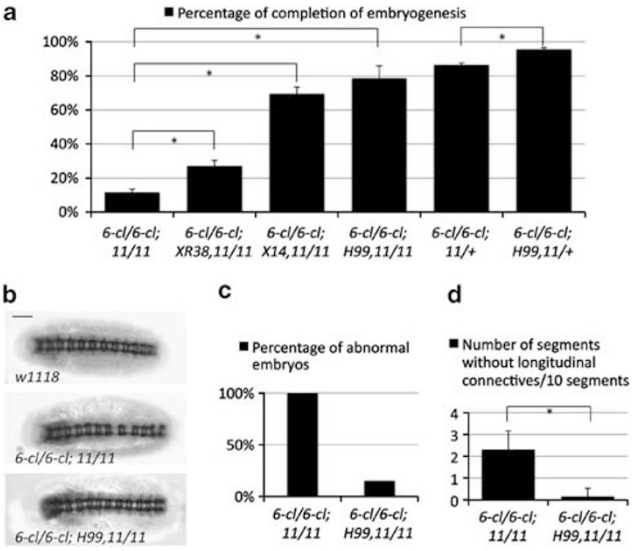

Figure 4 Suppression of the mutant phenotypes by reduced proapoptotic gene dosage. (**a**) Histogram showing percentage of embryos of the indicated genotypes that completed embryonic development. *XR38*, *11*; *XR14*, *11* and *H99*, *11* denote the recombinant chromosomes carrying the *miR-11* allele and the *Df(3L)X38*, *Df(3l)X14* and *Df(3L)H99* deletions, respectively. Error bars represent standard deviation from three independent experiments. * indicates that the differences were statistically significant, $P<0.05$ (Student's *t*-test). (**b**) Ventral views of embryos of the indicated genotypes labeled with antibody BP102. Scale bar: 50 μm. (**c**, **d**) Histograms showing quantification of the defects in the double mutant embryos *versus* double mutants carrying one copy of the *H99* deletion. (**c**) Percentage of embryos affected in at least one segment of the CNS. (**d**) Average number of affected segments per 10 embryo segments scored. Error bars represent standard deviation from at least 20 embryos. * indicates that the difference was statistically significant, $P<0.05$ (Student's *t*-test)

To ask whether the elevated expression of proapoptotic genes was sufficient to explain the embryonic lethality observed in the double mutant embryos, we made use of a set of chromosomal deletions that remove *hid*, *rpr*, *grim* and *skl*. *Df(3L)H99* removes *rpr*, *grim* and *hid*. *Df(3L)X38* removes *rpr* and *skl*. *Df(3L)X14* removes *hid*. Each of these deletions was recombined onto the *miR-11* mutant chromosome, and the recombinant chromosome was introduced into the *miR-11/miR-6* double mutant background. The *miR-6 miR-11*double mutant embryos carrying *Df(3L)X38* have only one copy of the *rpr* and *skl* genes, which should limit their ability to overexpress *rpr* and *skl*. This combination showed a statistically significant partial suppression of the lethality of the *miR-6 miR-11* double mutant embryos (Figure 4a). Removing one copy of *hid* in the *miR-6 miR-11* double mutant background using the *Df(3L)X14* recombinant produced strong suppression of the lethality (Figure 4a). Removing one copy each of *rpr, grim* and *hid* in the *miR-6 miR-11* double mutant background using the *Df(3L)H99* recombinant also produced strong suppression (Figure 4a). The *Df(3L)H99* recombinant also showed suppression of the milder lethal phenotype in the mutant combination lacking *miR-6* but having one copy of *miR-11* (Figure 4a).

We made use of the strong suppression provided by introducing the *Df(3L)H99* to examine the suppressed phenotype in more detail. The axonal scaffolding defects were suppressed in the embryonic CNS of the *miR-6 miR-11* double-mutant embryos carrying *Df(3L)H99* (Figure 4b). The percentage of double mutant embryos showing defects in the patterning of the embryonic CNS decreased from 100 to ~15% (Figure 4c), and the number of affected segments per embryo decreased from an average of 2 to ~0.2 (Figure 4d). These experiments provide evidence that the lethality observed in the *miR-6 miR-11* double mutants was caused by elevated proapoptotic gene expression, and show a correlation between the morphological defects in the CNS and lethality. They provide evidence that multiple proapoptotic genes can contribute to the lethality, but suggest that *hid* has a significant role.

Misregulation of proapoptotic genes in *miR-6/miR-11* double mutant embryos. The 3′UTRs of the proapoptotic genes, *rpr*, *grim*, *skl* and *hid* contain predicted binding sites for *miR-6* and *miR-11*. Depletion of *miR-6* in the embryo using antisense oligonucleotides has been reported to affect the expression of co-injected 3′UTR reporters for *hid*, *skl* and *rpr*, whereas depletion of *miR-11* affected *rpr*, *grim* and *skl* 3′UTR reporters.[27] To ask whether the effects of *miR-6* and *miR-11* were direct, we prepared luciferase reporters in which their predicted target sites were mutated. Coexpression of *miR-6* or *miR-11* with the intact *grim* reporter transgenes in S2 cells led to downregulation of luciferase activity (Figure 5a). In both cases mutation of the predicted site abrogated this downregulation. Coexpression of *miR-6* or *miR-11* with the intact *rpr* reporter transgenes in S2 cells led to downregulation of luciferase activity (Figure 5b). Again, mutation of the predicted site abrogated downregulation. The *skl* reporter has two predicted sites. This reporter was also downregulated by coexpression of *miR-6* or *miR-11* (Figure 5c). Mutation analysis showed that site 2 was functionally important, whereas mutation of site 1 had no effect. Comparable experiments using the *hid* 3′UTR reporter in S2 cells showed an unanticipated upregulation by both *miR-6* and *miR-11*. This was observed for the intact and the target-site mutant versions of the *hid* 3′UTR (data not shown). This suggests that the miRNAs indirectly alleviated repression of the *hid* 3′UTR reporters, perhaps as a consequence of regulating another target in the S2 cells. Using the full length 3′UTR, we cannot determine whether they directly affect *hid* regulation via the predicted sites. However, a recent report has provided independent evidence that miR-11 can function via smaller fragments of the *hid* 3′UTR containing the predicted sites.[36] These observations suggest that that *miR-6* and *miR-11* can each function via the identified sites in the 3′UTRs of *grim*, *rpr* and *skl* to regulate their expression.

Discussion

Multiple members of a miRNA family target the proapoptotic pathway. In this study, we have presented evidence that *miR-6 and miR-11* control apoptosis *in vivo*, through regulation of genes of the proapoptotic pathway. Limiting the capacity of the *miR-6/11* mutants to overexpress the proapoptotic genes was sufficient to rescue the mutants to viability and to restore normal patterning of the CNS. This suggests that the proapoptotic genes *rpr*, *grim*, *skl* and *hid*

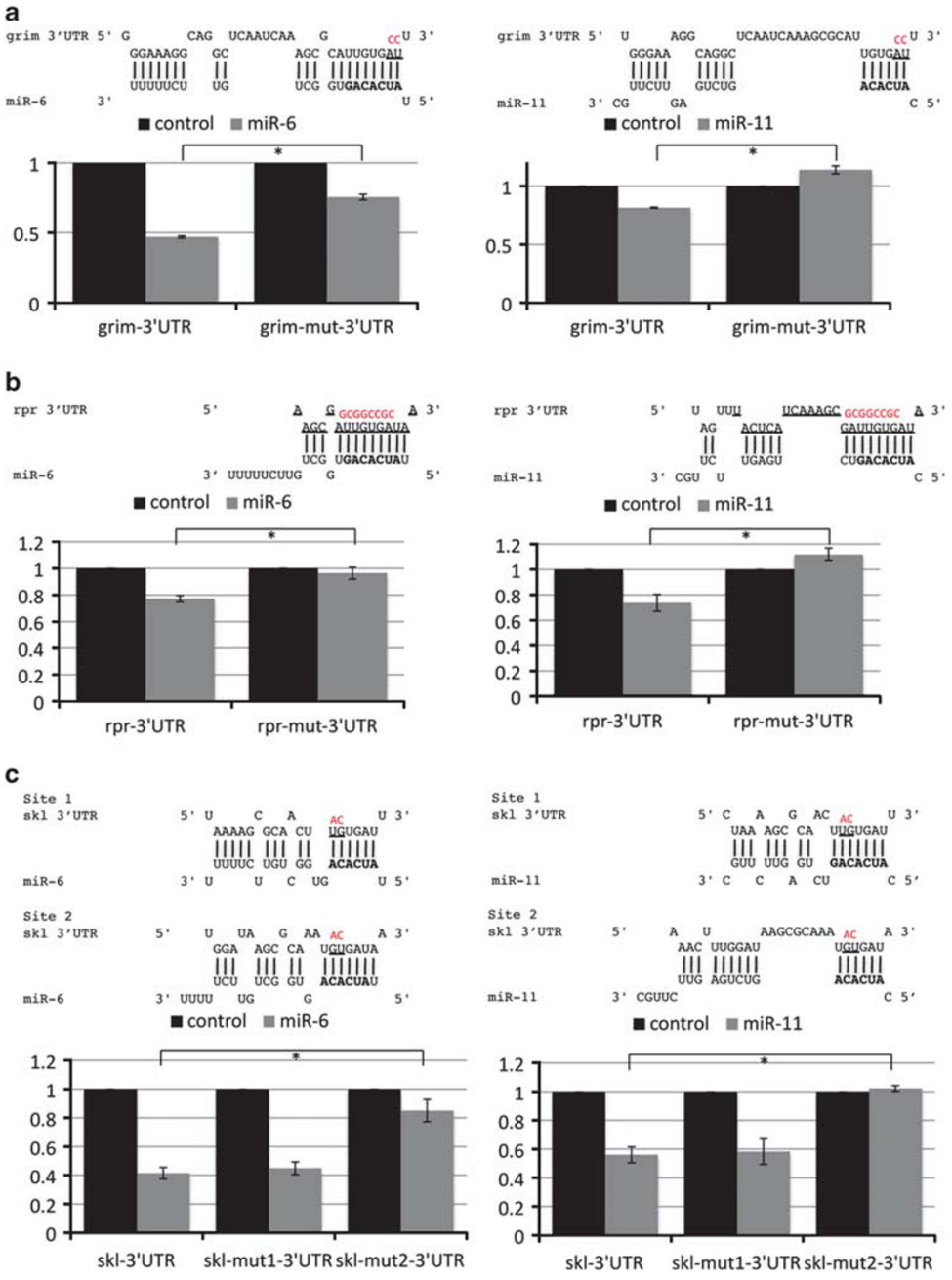

Figure 5 miRNA sites in the proapoptotic genes. (**a**) Regulation of the grim 3′UTR reporter by miR-6 (left panel) and miR-11 (right panel). Diagram illustrating the predicted pairing between the miRNAs and the predicted site in the grim UTR is shown above the histograms. Changes introduced into the seed region to destroy the binding site are shown in red. Histograms show the effect of coexpressed miR-6 or miR-11 on the luciferase activity from the reporter transgene with the intact (grim-3′UTR) or mutated target sites (grim-mut-3′UTR). Control samples were cotransfected with the empty miRNA vector and did not express the miRNA. Error bars represent standard deviation from three independent experiments. * indicates that the difference between the indicated pair was statistically significant, $P < 0.05$ (Student's *t*-test). (**b**) As in **a**, depicting the *rpr* 3′UTR and the corresponding luciferase assays. (**c**) As in **a**, depicting two sites in the *skl* UTR and the corresponding luciferase assays

are biologically significant targets through which *miR-6/11* functions *in vivo*.

It is noteworthy that the two miRNAs appear to have overlapping functions. They are coexpressed in the embryo, and removal of both is required to elicit a strong phenotype. Removing one copy of *miR-11* in the *miR-6* mutant background showed a slight effect, but the reciprocal combination did not. There are three copies of *miR-6* in the *miR-309* cluster[28] and based on miRNA sequence data, *miR-6* is considerably more abundant than *mR-11* at most stages of embryogenesis.[32] Consistent with this, expression from one copy of the *miR-6* locus is sufficient, whereas expression from one copy of *miR-11* is not quite sufficient to provide normal function. However, the observed 5–10 fold disparity in their relative copy number in total embryonic RNA might be misleading. It is possible that their activity levels are more

comparable in the developing embryonic CNS, where *miR-11* appears to be relatively more abundant. Tissue specific data on miRNA sequence levels would be needed to address this.

The miR-2 seed miRNA family has six other members, which might contribute to regulation of the proapoptotic genes. The ability of the *miR-2* and *miR-13* groups of miRNAs to regulate 3′UTR reporters for the proapoptotic genes has been demonstrated.[25–27] The roles of these miRNAs have been examined using injection of 2-*O*-methyl antisense oligonucleotides (antimirs) to deplete miRNA function in the embryo.[27] Injection of antimirs directed against *miR-6* was reported to cause severe apoptosis in embryos, with milder effects following injection of antimirs to *miR-11*. However, as reported here, mutants removing *miR-11* or removing *miR-6* miRNAs individually did not cause embryonic lethality (this work and Bushati *et al*[28]). Instead, we found that embryonic lethality and elevated apoptosis resulted in the double mutant combination that simultaneously removes both *miR-11* and *miR-6*. This lethality could be rescued by restoring expression of miRNA genetically. Assessment of the evidence suggesting that depletion of *miR-2* and *miR-13* group miRNAs results in embryonic apoptosis,[27] should await functional characterization of loss-of-function mutants that remove their functions *in vivo*.

Roles of miRNAs in embryonic CNS development. Apoptosis has a key role in pattern formation during development of the nervous system. Pruning of excess cells by apoptosis is central to the developmental of the CNS. In the developing retina, EGFR-mediated signaling selects cells to form ommatidia,[37] whereas excess cells are pruned through apoptosis.[38] Genetic analysis has shown that *rpr* is involved in the pruning of neuroblasts.[13] Regulated apoptosis of glia is also important in CNS patterning, as these cells contribute to the correct organization of the axon scaffold.[34] A subset of CNS midline glia cells undergoes apoptosis, resulting in selection of 3 cells per segment from initial pool of 10 cells. Cell interactions may provide trophic signals that support survival of these glia.[39]

Intriguingly, previous studies have shown that overexpression of *rpr* and *hid*, or *grim* in the midline glia leads to axon scaffold defects[40,41] that resemble those we have observed in the *miR-6/11* double-mutant embryo. The abnormal pattern of the axonal scaffold in *miR-6/11* double-mutant embryo might be due to loss of midline glia as a consequence of the failure to limit proapoptotic gene expression. These miRNAs may contribute to maintaining the balance between cell survival and apoptosis during patterning of the CNS in the embryo. It is possible that the other members of the miR-2 family of miRNAs have similar roles in other aspects of the CNS development, or in other tissues.

Materials and Methods

Fly strains and genetics. *Df(3L)H99*, *Df(3L)X38* and *Df(3L)X14* flies were provided by Kristin White. The *miR-6* genomic rescue transgene was made by cloning genomic fragments containing the promoter and miR-6 hairpin into site-specific integration vector pattB.[42] Primers for the promoter were 5′-TCGTT AACAGATCTGCGGCCGCAATTACAAAGAAACTTCGATTG-3′ and 5′-GAGTTGTG GACTTTAAACATTGCTATTCCAAACTTTAAGAC-3′, and for miR-6 hairpin 5′-ATG TTTAAAGTCCACAACTC-3′ and 5′-CGACACTAGTGGATCTCTAGAAGCTAAATAC CCATATTTATTG-3′.

Generation of microRNA knockout mutants. miRNA mutants were generated using homologous recombination-based ends-out gene targeting,[43] using vectors as described.[30] Briefly, homology regions flanking miR-11 were amplified and cloned into the targeting vector pW25-RMCE. Details of the targeting protocol are available on request (or see Chen *et al*.[44]). Two pairs of primers were used to amplify upstream and downstream flanking sequences:

upstream flank: 5′-GCGGCCGCAAATGCATCGTAGGCACCTC-3′ and 5′-GCG GCCGCAGAGGAGAGAGAGAGCGGAGA-3′

downstream flank: 5′-CCTGCAGGTGTTTTATTCGCGTGCTTTCT-3′ and 5′-CC TGCAGGTTTACAACCTTTCGGCCAAC-3′.

To generate *miR-11* rescue flies, a DNA fragment covering the *miR-11* hairpin was amplified with the following primers, 5′-CGGTCGACAGATCTATGTGAGGCG-CACTTG-3′ and 5′-CGGGATCCAATTAAACAAATTAAACAAAT-3′, cloned into the pIB-GFP vector to replace GFP.[29] *miR-11* was re-introduced into the targeted locus using the RMCE-based method as described.[30]

Examination of embryonic development phenotype. 0–6-h embryos were collected, and either plated on a fresh apple juice plate immediately or aged overnight before plating. GFP balancer was used for identifying mutant chromosome. Mutant embryos were selected by separating GFP-expressing embryos from GFP-negative embryos under a fluorescence microscopy. Percentage of completion of embryogenesis was determined by counting the number of hatching embryos that gave rise to first instar larvae after 48 h.

Cell culture and luciferase assays. S2 cells were grown at 25°C in Express five SFM (Invitrogen) supplemented with L-glutamine. *Rpr*, *grim*, *hid* and *skl* 3′UTR luciferase reporters and *miR-6* or *miR-11* expression plasmids were expressed under the control of the tubulin promoter. Details of the plasmids are available on request. S2 cells were transfected using Cellfectin (Invitrogen, Carlsbad, CA, USA) in 96-well plates with 80 ng of *miR-6* or *miR-11* expression plasmid or empty vector, 10 ng of firefly luciferase reporter plasmid and 10 ng of Renilla luciferase DNA as a control. Transfections were done with triplicate technical replicates in three independent experiments. Dual luciferase assays (Promega, Madison, WI, USA) were performed on the transfected cell at 60 h post transfection.

qRT-PCR. Total RNA was extracted from samples with TRIzol reagent (Invitrogen). Quantitative real-time PCR was performed using an ABI7500 fast real-time PCR machine (Applied Biosystems, Foster City, CA, USA). Taqman miRNA assay was used for miRNA qRT-PCR. Primer sets were obtained from Applied Biosystems. Reverse transcription was done on 10 ng of total RNA and miRNA levels were normalized to *u27*. For mRNA qRT-PCR, total RNA was treated with RNAse-free DNaseI. cDNA was synthesized by using oligo-dT primers and Superscript RT-III (Invitrogen). Samples were then treated with RNaseH and used for qRT-PCR with the ABI SYBR green system. Measurements of transcript level were normalized to *rp49*. The following primers were used for qRT-PCR:

rp49 : 5′-GCTAAGCTGTCGCACAAA-3′ and 5′-TCCGGTGGGCAGCATGTG-3′

e2f : 5′-ACAGCAACAGCAGCAGTGTC-3′ and 5′-TGATGGACACAAAGGCG ATA-3′

skl : 5′-ACCAGGAGCAACAAGTGAGC-3′ and 5′-GTGGCCTTTAGTTTGCT GGA-3′

grim : 5′-AGCAACAATCGCAACAACAG-3′ and 5′-CAGAAGATCTGGGCCAA AAG-3′

rpr : 5′-GAGCAGAAGGAGCAGCAGAT-3′ and 5′-GGACTTTCTTCCGGTCTT CG-3′

hid : 5′-CCTCTACGAGTGGGTCAGGA-3′ and 5′-CGTGCGGAAAGAACACA TC-3′.

Antibody labeling and *in situ* hybridization. Mouse monoclonal antibody BP102 (Developmental Studies Hybridoma Bank, DSHB, Iowa City, IA, USA) was used at 1 : 50. Mouse monoclonal antibody anti-wrapper (DSHB) was used at 1 : 10.

HRP-conjugated secondary antibody (Jackson Immunoresearch, West Grove, PA, USA) was used at 1 : 500. For immunohistochemical detection, a glucose–oxidase–DAB–nickel method[45] was used for visualization. Rabbit anti-Caspase3 antibody (Cell Signaling, Beverly, MA, USA) was used at 1 : 50. Chicken anti-GFP antibody (Abcam, Cambridge, UK) was used at 1 : 2000. Alexa Fluor 488 or 555-conjugated secondary antibodies (Molecular Probes, Eugene, OR, USA) were used at 1 : 250 or 1 : 500. Samples were imaged using a Zeiss LSM700 confocal microscope (Carl Zeiss, Jena, Germany), and images were taken and analyzed with

ZEN browser software (Carl Zeiss, Jena, Germany). To quantify cell death in the embryos, the 3D-reconstruction of confocal stacks was obtained with the 'isosurface' module of Imaris software (Bitplane AG, Zurich, Switzerland) and the total volume enclosed by the isosurface was measured. Light microscopy was performed with a Zeiss Imager M2 microscopy (Carl Zeiss, Göttingen, Germany) equipped with AxioCam HRc camera. Images were acquired and analyzed with AxioVision software (Carl Zeiss, Göttingen, Germany). miRNA primary transcript *in situ* hybridization was performed as described in Stark *et al.*[46] Primers used to generate pri-miR-11 probe were 5′- TAGTTGTAACGTATTGGCAAAG-3′ and 5′- TG ATTTTACATTGGGTTATTTG-3′, and primers used to generate pri-miR-6 were 5′- CA GTCGCCACCTATACAGTTTAAGG-3′ and 5′- TGCCACAACGAACTTCAATGG-3′.[28]

Conflict of Interest

The authors declare no conflict of interest.

Acknowledgements. We are grateful to Tan Kah-Junn and Song Shilin for their technical support and to Pushpa Verma and Xin Hong for their advice on the miRNA knockout and cell culture experiments. This work was supported by core funding from the Institute of Molecular Cell Biology and by EU-FP6 grant 'Sirocco' LSHG-CT-2006-037900.

1. Pelengaris S, Khan M, Evan G. c-MYC: more than just a matter of life and death. *Nat Rev Cancer* 2002; **2**: 764–776.
2. Hanahan D, Weinberg RA. Hallmarks of cancer: the next generation. *Cell* 2011; **144**: 646–674.
3. Huang J, Wu S, Barrera J, Matthews K, Pan D. The Hippo signaling pathway coordinately regulates cell proliferation and apoptosis by inactivating Yorkie, the Drosophila homolog of YAP. *Cell* 2005; **122**: 421–434.
4. Goyal L. Cell death inhibition: keeping caspases in check. *Cell* 2001; **104**: 805–808.
5. Moberg KH, Bell DW, Wahrer DC, Haber DA, Hariharan IK. Archipelago regulates Cyclin E levels in Drosophila and is mutated in human cancer cell lines. *Nature* 2001; **413**: 311–316.
6. Moberg KH, Mukherjee A, Veraksa A, Artavanis-Tsakonas S, Hariharan IK. The Drosophila F box protein archipelago regulates dMyc protein levels *in vivo*. *Curr Biol* 2004; **14**: 965–974.
7. Thompson BJ, Cohen SM. The Hippo pathway regulates the bantam microRNA to control cell proliferation and apoptosis in Drosophila. *Cell* 2006; **126**: 767–774.
8. Colombani J, Polesello C, Josue F, Tapon N. Dmp53 activates the Hippo pathway to promote cell death in response to DNA damage. *Curr Biol: CB* 2006; **16**: 1453–1458.
9. Kurada P, White K. Ras promotes cell survival in Drosophila by downregulating hid expression. *Cell* 1998; **95**: 319–329.
10. Bergmann A, Agapite J, McCall K, Steller H. The Drosophila gene hid is a direct molecular target of Ras-dependent survival signaling. *Cell* 1998; **95**: 331–341.
11. Brodsky MH, Nordstrom W, Tsang G, Kwan E, Rubin GM, Abrams JM. Drosophila p53 binds a damage response element at the reaper locus. *Cell* 2000; **101**: 103–113.
12. Zhou L, Steller H. Distinct pathways mediate UV-induced apoptosis in Drosophila embryos. *Dev Cell* 2003; **4**: 599–605.
13. Peterson C, Carney GE, Taylor BJ, White K. Reaper is required for neuroblast apoptosis during Drosophila development. *Development* 2002; **129**: 1467–1476.
14. Kornbluth S, White K. Apoptosis in Drosophila: neither fish nor fowl (nor man, nor worm). *J Cell Sci* 2005; **118**: 1779–1787.
15. Lin HV, Rogulja A, Cadigan KM. Wingless eliminates ommatidia from the edge of the developing eye through activation of apoptosis. *Development* 2004; **131**: 2409–2418.
16. Cordero J, Jassim O, Bao S, Cagan R. A role for wingless in an early pupal cell death event that contributes to patterning the Drosophila eye. *Mech Dev* 2004; **121**: 1523–1530.
17. Jiang C, Lamblin AF, Steller H, Thummel CS. A steroid-triggered transcriptional hierarchy controls salivary gland cell death during Drosophila metamorphosis. *Mol Cell* 2000; **5**: 445–455.
18. Loffler D, Brocke-Heidrich K, Pfeifer G, Stocsits C, Hackermüller J, Kretzschmar AK *et al.* Interleukin-6 dependent survival of multiple myeloma cells involves the Stat3-mediated induction of microRNA-21 through a highly conserved enhancer. *Blood* 2007; **110**: 1330–1333.
19. Seike M, Goto A, Okano T, Bowman ED, Schetter AJ, Horikawa I *et al.* MiR-21 is an EGFR-regulated anti-apoptotic factor in lung cancer in never-smokers. *Proc Natl Acad Sci USA* 2009; **106**: 12085–12090.
20. Yang CH, Yue J, Fan M, Pfeffer LM. IFN induces miR-21 through a signal transducer and activator of transcription 3-dependent pathway as a suppressive negative feedback on IFN-induced apoptosis. *Cancer Res* 2010; **70**: 8108–8116.
21. Hermeking H. The miR-34 family in cancer and apoptosis. *Cell Death Differ* 2010; **17**: 193–199.
22. Walker JC, Harland RM. microRNA-24a is required to repress apoptosis in the developing neural retina. *Genes Dev* 2009; **23**: 1046–1051.
23. Brennecke J, Hipfner DR, Stark A, Russell RB, Cohen SM. *bantam* encodes a developmentally regulated microRNA that controls cell proliferation and regulates the pro-apoptotic gene hid in Drosophila. *Cell* 2003; **113**: 25–36.
24. Hilgers V, Bushati N, Cohen SM. Drosophila microRNAs 263a/b confer robustness during development by protecting nascent sense organs from apoptosis. *PLoS Biology* 2010; **8**: e1000396.
25. Stark A, Brennecke J, Russell RB, Cohen SM. Identification of Drosophila microRNA targets. *PLoS Biol* 2003; **1**: E60.
26. Brennecke J, Stark A, Russell RB, Cohen SM. Principles of microRNA-target recognition. *PLoS Biol* 2005; **3**: e85.
27. Leaman D, Chen PY, Fak J, Yalcin A, Pearce M, Unnerstall U *et al.* Antisense-mediated depletion reveals essential and specific functions of microRNAs in Drosophila development. *Cell* 2005; **121**: 1097–1108.
28. Bushati N, Stark A, Brennecke J, Cohen SM. Temporal reciprocity of miRNAs and their targets during the maternal-to-zygotic transition in Drosophila. *Curr Biol* 2008; **18**: 501–506.
29. Bateman JR, Lee AM, Wu CT. Site-specific transformation of Drosophila via phiC31 integrase-mediated cassette exchange. *Genetics* 2006; **173**: 769–777.
30. Weng R, Chen YW, Bushati N, Cliffe A, Cohen SM. Recombinase-mediated cassette exchange provides a versatile platform for gene targeting: knockout of miR-31b. *Genetics* 2009; **183**: 399–402.
31. Duronio RJ, O'Farrell PH, Xie JE, Brook A, Dyson N. The transcription factor E2F is required for S phase during Drosophila embryogenesis. *Genes Dev* 1995; **9**: 1445–1455.
32. Ruby JG, Stark A, Johnston WK, Kellis M, Bartel DP, Lai EC. Evolution, biogenesis, expression, and target predictions of a substantially expanded set of Drosophila microRNAs. *Genome Res* 2007; **17**: 1850–1864.
33. Czech B, Malone CD, Zhou R, Stark A, Schlingeheyde C, Dus M *et al.* An endogenous small interfering RNA pathway in Drosophila. *Nature* 2008; **453**: 798–802.
34. Klambt C, Jacobs JR, Goodman CS. The midline of the Drosophila central nervous system – a model for the genetic analysis of cell fate, cell migration, and growth cone guidance. *Cell* 1991; **64**: 801–815.
35. Noordermeer JN, Kopczynski CC, Fetter RD, Bland KS, Chen WY, Goodman CS. Wrapper, a novel member of the Ig superfamily, is expressed by midline glia and is required for them to ensheath commissural axons in Drosophila. *Neuron* 1998; **21**: 991–1001.
36. Truscott M, Islam AB, Lopez-Bigas N, Frolov MV. mir-11 limits the proapoptotic function of its host gene, dE2f1. *Genes Dev* 2011; **25**: 1820–1834.
37. Freeman M. Reiterative use of the EGF receptor triggers differentiation of all cell types in the Drosophila eye. *Cell* 1996; **87**: 651–660.
38. Wolff T, Ready DF. Cell death in normal and rough eye mutants of Drosophila. *Development* 1991; **113**: 825–839.
39. Bergmann A, Tugentman M, Shilo BZ, Steller H. Regulation of cell number by MAPK-dependent control of apoptosis: a mechanism for trophic survival signaling. *Dev Cell* 2002; **2**: 159–170.
40. Zhou L, Schnitzler A, Agapite J, Schwartz LM, Steller H, Nambu JR. Cooperative functions of the reaper and head involution defective genes in the programmed cell death of Drosophila central nervous system midline cells. *Proc Natl Acad Sci USA* 1997; **94**: 5131–5136.
41. Wing JP, Zhou L, Schwartz LM, Nambu JR. Distinct cell killing properties of the Drosophila reaper, head involution defective, and grim genes. *Cell Death Differ* 1998; **5**: 930–939.
42. Bischof J, Maeda RK, Hediger M, Karch F, Basler K. An optimized transgenesis system for Drosophila using germ-line-specific phiC31 integrases. *Proc Natl AcadSci USA* 2007; **104**: 3312–3317.
43. Gong WJ, Golic KG. Ends-out, or replacement, gene targeting in Drosophila. *Proc Natl Acad Sci USA* 2003; **100**: 2556–2561.
44. Chen YW, Weng R, Cohen SM. Protocols for use of homologous recombination gene targeting to produce microRNA mutants in Drosophila. *Methods Mol Biol* 2011; **732**: 99–120.
45. Shu SY, Ju G, Fan LZ. The glucose oxidase-DAB-nickel method in peroxidase histochemistry of the nervous system. *Neurosci Lett* 1988; **85**: 169–171.
46. Stark A, Brennecke J, Bushati N, Russell RB, Cohen SM. Animal microRNAs confer robustness to gene expression and have a significant impact on 3′UTR evolution. *Cell* 2005; **123**: 1133–1146.